Managed Pressure Control of Deep Closed-Loop Well Construction and Operation

Eric van Oort[1], Pradeepkumar Ashok[1], Dongmei Chen[1], Amirhossein Fallah[1], Roman Shor[2]

[1]The University of Texas at Austin

[2]University of Calgary

Keywords

Managed Pressure Drilling, MPD, Closed Loop Geothermal Systems, CLGS

ABSTRACT

To allow drilling and exploitation of deep CLGS wells, an integrated managed pressure operation (MPO) concept is presented. An automatically controlled MPO system deployed during drilling and heat extraction / production phases can maintain wellbore integrity, avoid fluid contamination, control the pressure-volume-temperature (PVT) behavior of the working fluid, and enable an open-hole completion and controlled heat extraction in the lateral portion of the CLGS well. To demonstrate the feasibility of this concept, a new integrated thermal and hydraulic multi-phase flow model was developed. This model was coupled to an automated managed pressure control algorithm to control both the phase dynamics of the drilling or circulating fluid in the well, as well as hydraulic pressure in the well required to maintain wellbore stability of any open-hole sections. Simulations for deep CLGS well designs show that the developed simulation and control approach can describe and control the transient temperature dynamics and power generation in such wells.

1. General Introduction

Managed pressure drilling (MPD) techniques (Figure 1) provide a varied and versatile toolkit that has served as an important enabler for oil and gas well construction, particularly when drilling more challenging wells (Rehm et al., 2013). Main benefits derived from adoption of MPD techniques during well construction include:

- Negotiating downhole drilling margins (difference between fracture pressure and either pore pressure or mud pressure needed to prevent borehole shear failure, whichever of the latter two is higher) better, with ability to manipulate the equivalent circulating density (ECD) within the available margin.
- Simplifying casing schemes, by extending casing points and eliminating casing/liner strings.
- Avoiding NPT associated with well control, lost circulation, wellbore instability and differential sticking problems.
- Direct control over bottom-hole pressure (BHP), with fast ability to arrest kicks and circulating them out using the Driller's Method for well control and kick circulation.
- Early kick detection (EKD), through sensitive "delta-flow" measurements that sensitively compare well inflow and outflow rates.
- Ability to carry out dynamic pore pressure tests (DPPT) and dynamic formation integrity / leak-off tests (DFIT/DLOT) for determining the boundaries on the drilling margin.
- Higher ROP by drilling with a lower density clean fluid with reduced overbalance pressure, reducing chip hold-down
- Better cementations through the use of Managed Pressure Cementing (MPC), allowing reduction of circulating ECD's during mud displacement that minimizes risk of induced lost circulation

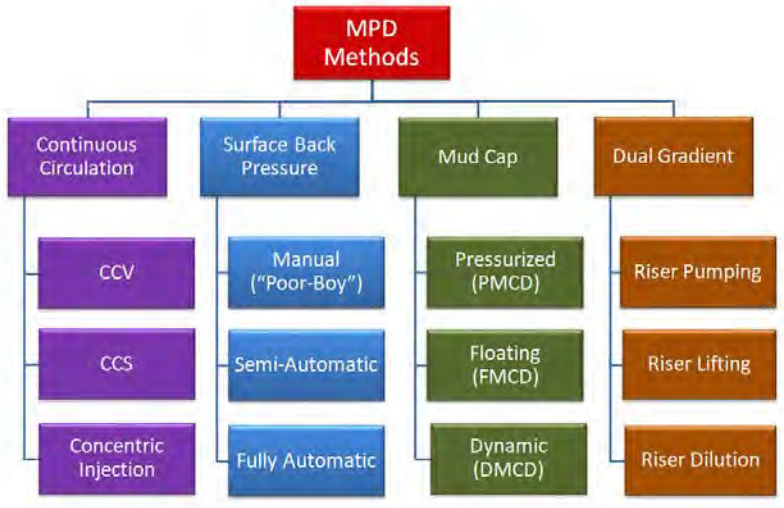

Figure 1 – Overview of MPD systems, with the 4 major "families" categorized as continuous circulation, surface back-pressure, mud cap drilling, and dual gradient (for offshore applications).

The MPD well construction benefits extend to geothermal drilling as well, and it is quite surprising that there have been so few applications of MPD in the geothermal domain to date (for some recent examples, see Pinkstone et al. (2018); Petrie and Doll (2021)). The following benefits are expected from more wide-scale adoption of MPD techniques in the geothermal well construction domain:

- Continuous Circulation (CC) allows fluid circulation without interruption, even when making drillstring connections. This technique creates a stable temperature and ECD profile in the annulus. This minimizes annular pressure fluctuations and associated "fatigue-cycling" on the borehole wall that may cause instability. It also allows the well to be drilled with a hydrostatically underbalanced fluid becoming overbalanced by continuous circulation. Hole cleaning is greatly improved, and the risk of pack-off-related stuck pipe incidents during connections is eliminated. Last-but-not least, cooling of downhole tools is greatly improved because fluid circulation is never stopped and the wellbore annulus is never allowed to re-heat.

- Surface Back-Pressure (SBP) comes with multiple benefits mentioned before, including EKD, ability to perform DPPT, DFIT and DLOT measurements, active well control response, ability to carry out MPC, etc. It can be used as an effective tool in managing wellbore stability and mitigating lost circulation, a significant challenge in most GT well construction projects. An important secondary benefit often observed when adopting SBP is a noticeable increase in rate of penetration (ROP), because light, clean fluids can often be used (with added back-pressure providing the additional contribution to the desired BHP not provided by the limited hydrostatic head of the fluid) that minimize chip hold-down.

- Mud Cap Drilling (MCD) techniques have been developed in oil and gas for dealing with severe lost circulation challenges when dealing with in-situ fractured formations, high vugular formations, karsts, etc. Rather than drilling blind, which provides no control and may present significant safety risks, pressurized mud cap drilling (PMCD) in particular yields a controlled operation with no mud returns or formation fluids/gases ever coming to surface. This is particularly important when gas-bearing zones (containing H_2S, CO_2, hydrocarbon gases) are intersected that present well control and associated safety risks. PMCD can be simply implemented when using SBP functionality at the rigsite, because the hardware required for the two operations (SBP and PMCD) is the same. The only major changes are the availability and use of sacrificial fluid (SAC, usually freshwater or seawater) for drilling and light annular mud (LAM) for annular control.

- Dual Gradient Drilling (DGD) techniques have been developed for simplification and efficiency improvement in offshore deepwater drilling. Although a far stretch at present, one may foresee a time when GT wells are drilled offshore in very deep water (e.g. along the mid-Atlantic ridge and the Pacific Ring of Fire) in a "not-in-my-backyard" fashion, benefiting from the adoption of DGD techniques. DGD implementation in both ECD reduction and full-DGD modes have the ability to significantly reduce deepwater well construction, with estimates up to ~40% time and cost reduction.

In the following, we will exclusively focus on the surface back-pressure (SBP) MPD variant in both the drilling phase as well as the operations phase for deep closed loop geothermal systems (CLGS).

2. Surface Back-Pressure MPO

The previous section argues that there are tangible benefits associated with considering MPD techniques for use in GT well construction. The use of SBP-MPD, however, may not be limited to the drilling phase but could be extended to the well operation during which heat extraction takes place, particularly for CLGS wells. Manipulation of the back-flow valve on a GT well is nothing new, but in the following we propose to perform this manipulation in an automated way to achieve certain purposes, particularly when using an open-hole completion in the well with high-temperature formations directly exposed to heat-exchanging circulating fluid. We have termed such use of SBP-MPD in the operations phase "managed pressure operations" (MPO). With MPO, bottomhole pressure (BHP) can be actively managed and automatically controlled for:

(1) Phase control of heat exchanging fluid returning to surface, e.g., preventing water from flashing to steam in the wellbore;

(2) Control of thermosiphon effect, which has a natural tendency to reduce the BHP which potentially could cause wellbore instability under certain circumstances; and,

(3) Allowing the exertion of additional BHP on open-hole formations to mechanically support the wellbore to prevent failure or thermally induced creep behavior in case of open hole completions. The latter assumes, of course, that the open-hole formations require such borehole stability / creep-mitigation support under the prevailing in-situ stress, pore pressure and temperature conditions.

Fluid phase behavior can be straightforwardly modeled by considering the thermodynamic behavior of the fluid under different pressure and temperature conditions, as has been done for water in Section 3. The thermosiphon effect can be modeled with a hydraulic model that considers the effects of temperature and pressure on fluid density. The wellbore stability requirements can be determined using appropriate rock mechanical failure modeling, considering wellbore characteristics (depth, deviation, azimuth), the in-situ stress tensor, the pore pressure (if present) as well as formation strength (Young's modulus, Poisson's ratio) and rock failure parameters (unconfined compressive strength (UCS), cohesion, friction angle) as inputs. An example of such modeling for the thresholds for shear failure (using the Modified Lade criterion, Ewy (1999)) and tensile failure, as well as their difference, is shown in Figure 2. This example considers the stability of a hard, normally pressured formation (loosely based on KTB amphibolite, see Haimson and Chang, 2002) at 7 km TVD in a strike-slip faulting environment, with modeling parameters as given in Table 1.

Table 1 – Overview of rock mechanical modeling parameters used for Figure 2.

Variable	***Value***	***Variable***	***Value***
Young's Modulus E	68.8 GPa	Maximum Horizontal Stress S_{Hmax} and azimuth	200 MPa, 60 degrees
Poisson's Ratio ν	0.26	Maximum Horizontal Stress S_V	158 MPa
UCS	68.6 MPa	Minimum Horizontal Stress S_{hmin}	132 MPa
Friction Coefficient	0.6	Pore Pressure	72.1 MPa

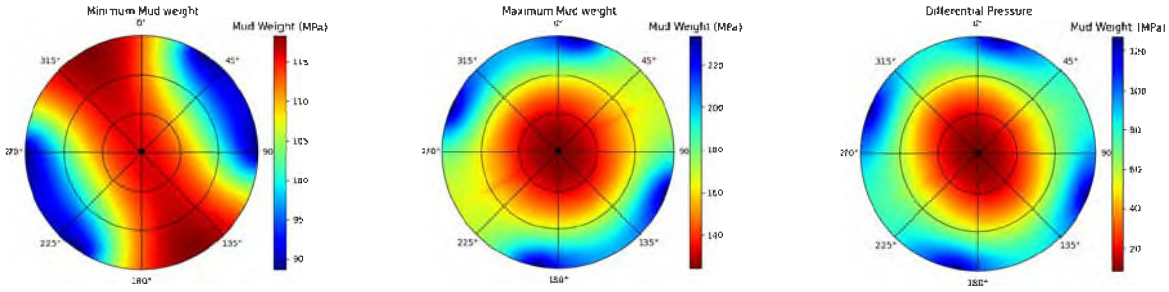

Figure 2 – Wellbore stability modeling for the parameters given in Table 1, with (left) minimum borehole fluid pressure to prevent shear failure according to the modified Lade criterion, (middle) fluid pressure to initiate tensile failure and fracturing, (right) difference plot, showing the available drilling margin.

Figure 2 shows that in this case, wellbore stability requires a borehole fluid pressure higher than the hydrostatic pressure of water (72.1 MPa), which can be managed using a higher density circulating fluid and/or active back-pressure from surface applied through SBP-MPD. Note that maintaining a wellbore overbalance pressure in the wellbore, however, can lead to time-delayed failure due to mud pressure penetration, which raises the near-wellbore pore pressure (even in tight rock with very low permeabilities) and lowers the near-wellbore effective stresses, driving the stress state towards the failure envelope over time. Such time-delayed failure was experienced during the drilling of the KTB well in Germany (see Azzola et al. 2019, Borm et al. 1997). KTB amphibolite was shown to have a very low permeability (van Oort, 1996) on the order of 0.1 nD (10^{-22} m^2); however, even at such low permeability the effects of mud pressure transmission still resulted in wellbore instability. The mechanism is shown graphically in Figure 3. Time-delayed failure can be prevented by hermetically sealing the borehole wall and plugging all permeability, e.g., by chemical means, thereby preventing any pressure communication between the wellbore and the adjacent formation.

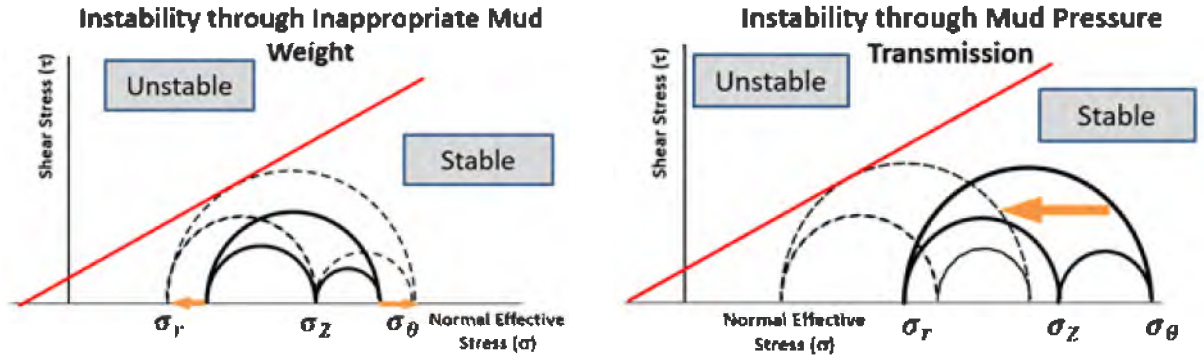

Figure 3 – Instability in tight, low-permeability formations can be triggered by (left) insufficient mud weight support (radial effective stress σ_r too low or reduced e.g. by swabbing the well), or (right) mud pressure transmission raising near-wellbore pore pressure, reducing effective stresses, and driving the stress state over time towards failure. Red line shows a linearized Mohr-Coulomb failure envelope.

3. MPO Model Description

An integrated thermal and hydraulic model using transient conservation equations was used to simulate dynamic well temperature profiles and SBP requirements. Details can be found in Fallah et al. (2019, 2021). The conservation equations are derived from the transient Navier-Stokes equations for pipe flow and account for turbulent friction forces, liquid compressibility, and temperature-dependent water properties:

$\frac{\partial \rho}{\partial t}$ $\frac{\partial \rho v}{\partial x}$ $\dot{m}_{source}$ .....(1)

$\frac{\partial \rho v}{\partial t}$ $\frac{\partial \rho v^2}{\partial x}$ $-\frac{\partial p}{\partial x}$ f_g f_w $\dot{M}_{source}$ .....(2)

$\frac{\partial \rho\ e+\frac{1}{2}v^2+gz}{\partial t}$ $\frac{\partial \rho v\ h+\frac{1}{2}v^2+gz}{\partial x}$ $\frac{\partial}{\partial x}\left(k\frac{\partial T}{\partial x}\right)$ $\dot{q}_{wall}$ $\dot{H}_{source}$ .....(3)

where t is time, x is the length along the direction of the well (measured depth, MD), ρ is density, v is velocity, $\dot{m}_{source}$ is the rate of mass generation per unit volume from sources, p is pressure, f_g is gravitational force per unit volume, f_w is wall friction per unit volume, $\dot{M}_{source}$ is the rate of momentum generation per unit volume from sources, e is the internal energy, g is the gravitational acceleration, z is the vertical depth, h is enthalpy, k is thermal conductivity, T is temperature, $\dot{q}_{wall}$ is the rate of external heat transfer per unit volume through the walls, and $\dot{H}_{source}$ is the rate of enthalpy generation per unit volume from sources. Internal energy and enthalpy are defined as:

e $\int_{T_0}^{T} c_v\ T\ dT$ e_0 .....(4)

h e p ρ.....(5)

where c_v is the specific heat capacity at constant volume, and T_0 and e_0 are the reference temperature and internal energy. The gravitational force and wall friction terms in the momentum equation are calculated as:

f_g $\rho g \cos(\theta$ .....(6)

f_w $-\frac{1}{2}\frac{f_D \rho v^2}{D}$ .....(7)

where θ is the hole deviation from the vertical direction, f_D is the Darcy-Weisbach friction factor, and D is the hole diameter. The external heat transfer in the energy equation between the rock formation flow and heat exchanging fluid in the wellbore, which are separated by casing and cement for cased-hole sections and are in direct contact for open-hole sections, is calculated using a heat transfer network discussed by Fallah et al. (2021). The boundary conditions used to solve Eqs. (1-3) include the pump rate and inlet temperature at the wellbore inlet, as well as the wellbore outlet pressure which is controlled by the automated MPO system. The inlet pressure, output flow rate, and outlet temperature are calculated numerically. The formation rock is discretized radially to account for the formation temperature dynamics in close vicinity of the well. Only the radial heat conduction inside the formation rock is considered due to the negligible temperature gradients in the axial direction. The heat transfer between the wellbore and the first formation node is calculated as:

$$\dot{q}_{wall} \quad \frac{T_1 - T_w}{R} \quad (8)$$

where T_1 is the temperature of the first formation cell, T_w is the temperature of the water in the well, and R is the thermal resistance. Total thermal resistance is calculated by summing the individual resistances between the water and the first cell (i.e. convection in the water, conduction through the casing and cement (which is zero in open-hole), and conduction in the formation rock). The heat transfer between the adjacent formation cells is calculated similarly, where the resistance is only the conduction resistance through the rock. Each individual conduction or convection resistance is calculated as:

$$R_{conduction} \quad \frac{A \ln \frac{r_o}{r_i}}{2\pi k_s} \quad (9)$$

$$R_{convection} \quad \frac{A}{h\pi D} \quad (10)$$

where A is the cross-sectional area of the well, r_o and r_i are the outer and inner radius of the solid across which heat is being conducted, k_s is the conductivity of the solid, is the diameter of the wall at which heat is being convected, and h is the convection coefficient. The convection coefficient is defined as:

$$h \quad \frac{Nu\, k}{D} \quad (11)$$

where k is the conductivity of water, D is the diameter of the hole, and Nu is the Nusselt number calculated from Eq. (12)**:**

$$Nu \quad \begin{cases} laminar\ flow \\ \dfrac{\left(\frac{f}{8}\right) Re - 1000\ Pr}{1 + 12\,7\left(Pr^{\frac{2}{3}} - 1\right)\sqrt{\frac{f}{8}}} \quad turbulent\ flow \end{cases} \quad (12)$$

where Re and Pr are the Reynolds number and Prandtl number, respectively.

Considering freshwater as the closed loop circulation and heat exchanging fluid, fitted polynomial models of water properties are used to calculate the density, viscosity, specific heat capacity at constant pressure and constant volume, and thermal conductivity. Density is modeled by a first-order polynomial function of pressure combined with a second-order polynomial function of temperature as:

$$\rho \quad \frac{p}{1490\ 9} - \quad * T^2 - \quad * T \quad (13)$$

where pressure is measured in Pa, temperature in ℃, and density in kg/m^3. Neglecting the effect of pressure, the viscosity, specific heat capacities, and thermal conductivity are assumed to be functions of temperature and are modeled as:

$$\mu \quad \begin{cases} * \ ^{-11} * T^4 - \ * \ ^{-9} * T^3 \ * \ ^{-7} * T^2 - \ * \ ^{-5} * T \ * \ ^{-3} & T \quad ℃ \\ - \ * \ ^{-11} * T^3 \ * \ ^{-8} * T^2 - \ * \ ^{-6} * T \ * \ ^{-4} & T \geq \quad ℃ \end{cases} \quad (14)$$

$$c_p \quad * \ ^{-4} * T^3 - \ * \ ^{-2} * T^2 \ * T \ * \ ^3 \quad (15)$$

$$c_v \quad * \ ^{-5} * T^3 - \ * \ ^{-2} * T^2 - \ * T \ * \ ^3 \quad (16)$$

$$k \quad - \ * \ ^{-6} * T^2 \ * \ ^{-3} * T \ * \ ^{-1} \quad (17)$$

where temperature is measured in ℃, viscosity in Pa.s, specific heat capacities in J/Kg.K, and thermal conductivity in W/m.K. Details of the semi-implicit numerical scheme and the discretization of Eqs. (1-3), as well as the validation of the discretization method are based on the method proposed by Evje and Fjelde (2002), with details given in Fallah et al. (2021). A polynomial fit of water pressure as a function of temperature is presented in Eq. (18). The boiling pressure monotonically increases with the temperature. At any given temperature, water starts boiling if the pressure is below the boiling pressure threshold.

$$p_{boil} \quad * \quad ^{-3} * T^4 - \quad * \quad ^{-1} * T^3 \quad * \quad ^{1} * T^2 - \quad * \quad ^{3} * T \quad * \quad ^{4} \text{.....(18)}$$

In Eq. (18), temperature is measured in ℃ and pressure in Pa. Deep in the wellbore itself, the hydrostatic pressure of the water column applies sufficient pressure to avoid boiling downhole, even for extreme temperature gradients and high absolute downhole temperatures. The well location where boiling is most likely to occur is on surface at the outlet due to the reduced hydrostatic pressure. Therefore, a proportional integral (PI) controller that enables MPO was designed to maintain SBP above the boiling pressure by automatic choke opening adjustment. The MPO system controls the fluid PVT behavior, maintains pressure control across the open lateral, ensures well integrity, and avoids reservoir influxes and fluid contamination. Simulating the automated choke control behavior relies on capturing the pressure wave dynamics and the fast transients associated with rapid choke adjustments. We simulate choke opening manipulation such that:

$$p_{SBP} \quad p_{boil}\ T \quad SM \quad for\ p_{boil}\ T \quad p_{BHS} - p_{hydrostatic} \text{ .....(19A)}$$

$$p_{SBP} \quad p_{BHS} - p_{hydrostatic} \quad SM \quad for\ p_{boil}\ T \quad p_{BHS} - p_{hydrostatic} \text{.....(19B)}$$

where p_{SBP} is the SBP that is maintained by the choke, $p_{boil}\ T$ is the boiling pressure on surface (which is a function of the outlet temperature), and p_{BHS} is the BHP required for borehole stability of creep control, $p_{hydrostatic}$ is the hydrostatic head of the circulating fluid, and SM is an additional safety margin (this margin was set to a nominal 1 MPa for the simulation presented below). The control strategy outlined in Eqs.(19) is simple and straightforward, with a controller being informed by temperature measurement of the fluid exiting the well and wellbore stability information obtained before and potentially during the drilling phase. It could, however, be made more robust with digital twinning of the circulation operation and taking advanced effects such as the influence of a changing temperature on wellbore stability into account.

4. Simulation Results

The above model is illustrated here for a U-shaped closed loop well with 7 km TVD and a 5 km long connecting lateral section. The diameter of the open-hole lateral section is 31.115 cm (12.25 in) and the build radius of the curve sections of the well is assumed to be 200 m. Water is pumped at 300 m^3/h into a U-shaped well for 13 hours, followed by a 3-hour pumping at 400 m^3/h, and 4 hours of pumping at 350 m^3/h, for a total circulation time of 20 hours. The initial temperature of the water in the well is assumed to be equal to the temperature profile of the surrounding rock, linearly increasing from 40 ℃ at surface to 250 ℃ at 7 km TVD. The density, heat capacity, and thermal conductivity of the rock formation are set to be 2700 kg/m^3, 1000 J/kg.K, and 2.5 W/m.K, respectively, representing average crust properties. During the simulation, an automatic controller is used to apply enough backpressure to avoid water evaporation and associated pressure reduction in the well. The inlet vertical sections are cased

and cemented using 33.973 cm outer diameter casing. Casing and cement thicknesses for the cased sections are set to be 1 cm and 2.5 cm, respectively.

Fig. 4 shows the water, rock formation, and initial temperatures versus MD at different times. The water temperature is initially assumed to be in thermal equilibrium with the rock formation (e.g., after an extended shut-in period of no circulation). When pumping starts, high-temperature water in the horizontal section is pumped out of the well and replaced by cold water from the inlet section of the well. After continuing pumping for a few hours, a semi-steady-state is reached where all the water is displaced by the cold water from the inlet section of the well. During the process, the surrounding rock temperature continues to decrease due to the heat transfer to the water. (i.e., thermal depletion of the well). As the water is circulated up in the return section, the decreasing temperature of the surrounding rock (due to the thermal gradient) cause a heat loss from the water to the cold rock formation. The maximum gradient in the temperature profile is observed at the beginning of the horizontal section, where the temperature difference between the water and un-cased formation is at a maximum. It is observed that the increased pump rate between 13 and 16 hours into the simulation reduces the temperature profile along the well. This is because with the increased pump rate and fluid velocities within the wellbore, water has less time to be heated up as it moves along the well. When the pump rate is reduced at 16 hours, the fluid temperature increases again due to the reduced velocities in the well. However, the effect of lower fluid velocities is offset by the continuous thermal depletion of the surrounding rock.

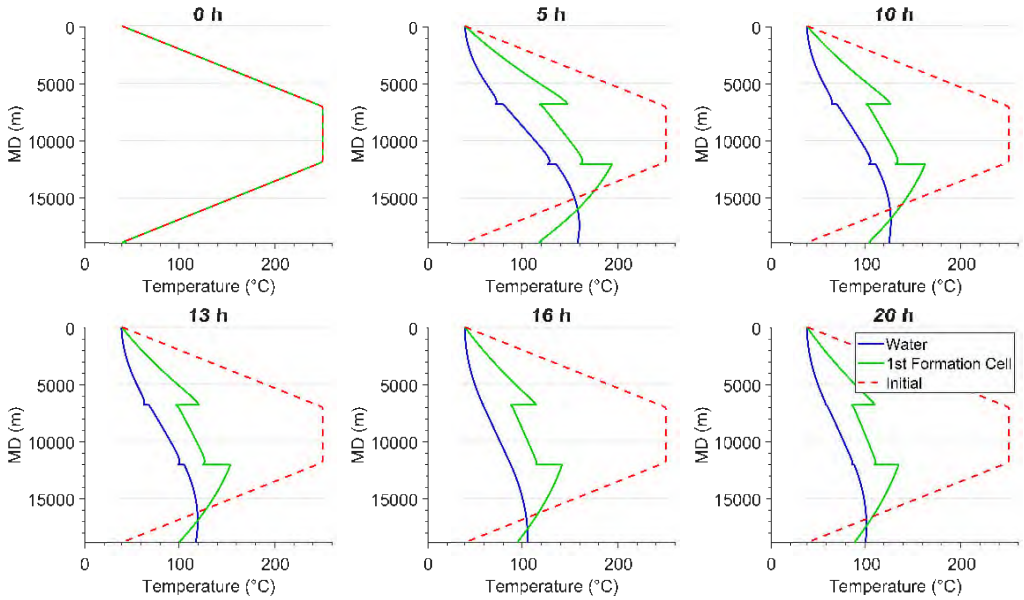

Figure 4 - Temperature profile at different times during well operation.

Fig. 5 shows the outlet temperature, net thermal power generation, and outlet flow rate. **Fig. 6** shows the SBP and choke opening versus time. As the outlet temperature increases between 0-134 min, the boiling pressure increases according to Equation (18). The automated controller calculates the boiling pressure, adjusts the choke opening, and applies sufficient SBP to avoid evaporation and maintain well control. A maximum SBP of 2.4 MPa is applied at 134 minutes when the exit temperature peaks. As the temperature and boiling pressure decrease, the choke is

slowly opened to reduce unnecessary excess SBP, while maintaining a safety margin of 1 MPa (assuming that no excess safety margin is required for open-hole stability control in the horizontal lateral). Varying the pump rate will affect the outlet temperature, and the choke is automatically adjusted to maintain the 1 MPa safety margin while the boiling pressure varies.

5. Conclusions

Although MPD techniques have not yet found widespread application in GT well construction, the case is made in this paper to consider all forms of MPD (continuous circulation, surface back-pressure, mud cap drilling, and potentially even dual gradient drilling for future offshore deepwater GT wells) for GT well construction due to tangible benefits that can make operations safer and more efficient, thereby lowering drilling costs. MPD offers new ways of dealing with well control, borehole instability and stuck pipe, lost circulation control etc. to be yet fully explored in the GT domain. In addition, there may be an opportunity to use SBP-MPD control methodologies in the well operation / heat extraction phase of closed loop wells as well, by offering automated choke control that can handle phase behavior control and thermosiphon control of the circulating fluid, as well as borehole stability management of any open hole formations. This type of control is illustrated here using a representative example for a 7 km TVD well using a comprehensive hydraulics model coupled with a thermal model.

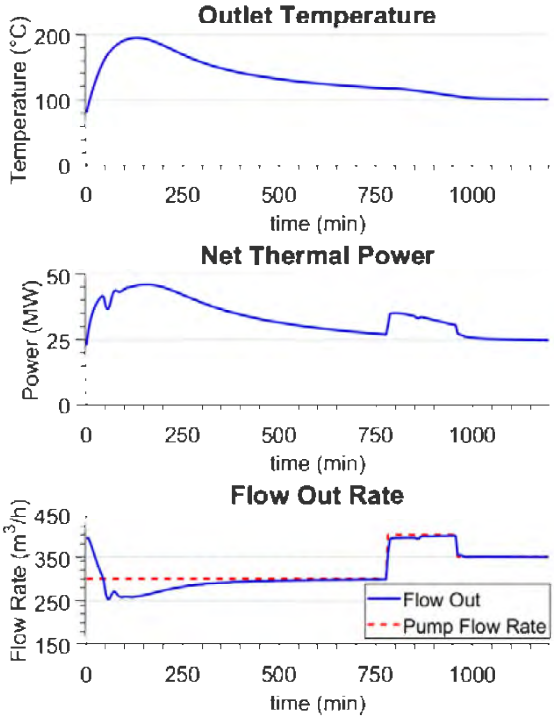

Figure 5 - Outlet temperature, thermal power and outlet flow versus time.

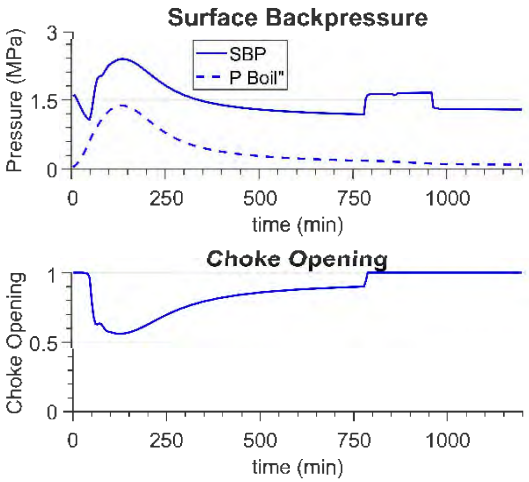

Figure 6 - SBP and choke opening versus time.

Acknowledgement

This work was carried out under the auspices of the RAPID consortium at the University of Texas at Austin, and we thank the 2021 RAPID sponsors (Baker Hughes, Cenovus, ConocoPhillips, Eavor, Halliburton, Hess, H&P, JOGMEC, Nabors, NOV, Oxy, and Saudi Aramco) for their support and guidance.

REFERENCES

Azzola, J., Valley, B., Schmittbuhl, J., & Genter, A. (2019). “Stress characterization and temporal evolution of borehole failure at the Rittershoffen geothermal project”. *Solid Earth, 10(4),* 1155-1180.

Borm, G., Engeser, B., Hoffers, B., Kutter, H.K., Lempp, C., (1997). “Borehole instabilities in the KTB main borehole”. *J. Geophys. Res.: Solid Earth 102 (B8),* 18507–18517. doi:10.1029/96JB03669.

Evje, S, Fjelde, KK, (2002). “Relaxation schemes for the calculation of two-phase flow in pipes”. *Math Comput Model 36*: 535–67. https://doi.org/10.1016/S0895-7177(02)00182-6.

Ewy, R.T., (1999). "Wellbore-Stability Predictions by Use of a Modified Lade Criterion." *SPE Drill & Compl 14*: 85–91. doi: 10.2118/56862-PA

Fallah A, Gu Q, Ma Z, Karimi Vajargah A, Chen D, Ashok P, et al. (2019). “An integrated thermal and multi-phase flow model for estimating transient temperature dynamics during drilling operations”. *Society of Petroleum Engineers*. doi:10.2118/194083-MS.

Fallah, A., Gu, Q., Chen, D., Ashok, P., & van Oort, E. (2021). “Globally scalable geothermal energy production through managed pressure operation control of deep closed-loop well systems”. *Energy Conversion and Management, 236,* 114056.

Haimson, B. C., & Chang, C. (2002). “True triaxial strength of the KTB amphibolite under borehole wall conditions and its use to estimate the maximum horizontal in situ stress”. *Journal of Geophysical Research: Solid Earth, 107(B10), ETG-15*.

Petrie, S.W., and Doll, R. (2021) "Using Continuous Circulation in Geothermal Wells to Improve Drilling Performance and Reduce NPT Related to Wellbore Stability." *Society of Petroleum Engineers*. doi: https://doi.org/10.2118/204046-MS.

Pinkstone, H., McCluskey, T., MacGregor, A., Scagliarini, S., & Indrinanto, Y. 2018. Using Drill Pipe Connection Continuous Circulation Technology on a Geothermal Drilling Project in Indonesia to Reduce Stuck Pipe Events. *Society of Petroleum Engineers*. doi:10.2118/191074-MS.

Rehm, B., Schubert, J.J., Haghshenas, A., Paknejad, A.S., and Hughes, J. (2013). *Managed Pressure Drilling*. Elsevier.

van Oort, E. (1994) "A Novel Technique for the Investigation of Drilling Fluid Induced Borehole Instability in Shales." *Rock Mechanics in Petroleum Engineering, Delft, Netherlands.* doi: 10.2118/28064-MS

Zhao, Y., Feng, Z., Xi, B., Wan, Z., Yang, D., & Liang, W. (2015). “Deformation and instability failure of borehole at high temperature and high pressure in hot dry rock exploitation”. *Renewable Energy, 77,* 159-165.